*nect Conference*, p. 373, Santa Clara, CA, IEEE (1989).

16. T. Iwamori, Y. Sakata, H. Kojima, and Y. Yatsuda, *ASTM Spec. Tech. Publ.*, 252 (1989).
17. H. Kojima, T. Iwamori, Y. Sakata, T. Yamashita, and Y. Yatsuda, in *Proceedings of 1988 IEEE VLSI Multilevel Interconnect Conference*, p. 390, Santa Clara, CA, IEEE (1988).
18. M. Kawai, K. Matsuda, K. Miki, and K. Sakiyama, *ibid.*, p. 419.
19. S. K. Gupta, *Mater. Res. Soc. Symp. Proc.*, **108**, 275 (1988).
20. J. C. Debsikdar, *Adv. Ceram. Mater.*, **1**, 93 (1986).
21. B. E. Yoldas, *J. Non-Cryst. Solids*, **51**, 105 (1982).
22. H. Schmidt, H. Scholze, and A. Kaiser, *ibid.*, **63**, 1 (1984).
23. C. Chiang and D. B. Fraser, in *Proceedings of 1989 IEEE VLSI Multilevel Interconnect Conference*, p. 397, Santa Clara, CA, IEEE (1989).
24. R. J. Hopkins, T. A. Baldwin, and S. K. Gupta, in *ULSI Science and Technology/1989*, C-M. Osburn and J. M. Andrews, Editors, PV 89-9, p. 530, The Electrochemical Society Proceedings Series, Pennington, NJ (1989).
25. G. E. Whitwell and T. E. Wade, in *Proceedings of 1987 IEEE VLSI Multilevel Interconnect Conference*, p. 292, Santa Clara, CA, IEEE (1987).
26. S. Ito, Y. Homma, and E. Sasaki, *This Journal*, **137**, 1212 (1990).
27. M. P. Woo, J. L. Cain, and C.-O. Lee, *ibid.*, **137**, 196 (1990).
28. P. L. Pai, A. Chetty, R. Roat, N. Cox, and C. Ting, *ibid.*, **134**, 2829 (1987).
29. T. Nakano and T. Ohta, *ibid.*, Submitted for publication.
30. F. A. Leon, *IEEE Trans. Computer-Aided Design*, **CAD-7**, 168 (1988).
31. H. G. Tompkins and C. Tracy, *This Journal*, **136**, 2331 (1989).
32. N. Hirashita, I. Aikawa, T. Ajioka, M. Kobayakawa, F. Yokoyama, and Y. Sakaya, *IEEE IRPS*, 216 (1990).
33. N. Lifshitz, W. Y. C. Lai, and G. Smolinsky, *IEEE Electron Device Lett.*, **EDL-10**, 562 (1989).
34. D. Pramanik, S. Nariani, and G. Spadini, in *Proceedings of 1989 IEEE VLSI Multilevel Interconnect Conference*, p. 454, Santa Clara, CA, IEEE (1989).
35. B. Vollmer, G. Roeska, and J. Winnerl, *J. de Physique*, **49**, C4-311 (1988).
36. C. Chiang, N. V. Lam, J. K. Chu, N. Cox, D. Fraser, J. Bozarth, and B. Mumford, in *Proceedings of 1987 IEEE VLSI Multilevel Interconnect Conference*, p. 404, Santa Clara, CA IEEE (1987).
37. S. M. Sze, in *VLSI Technology*, 2nd ed., p. 157, McGraw-Hill, Inc., New York (1988).
38. C. H. Ting, N. Cox, R. Roat, P. L. Pai, and A. Chetty, in *Multilevel Metallization, Interconnection, and Contact Technologies*, L. B. Rothman and T. Herndon, Editors, PV 87-4, p. 209, The Electrochemical Society Proceedings Series, Pennington, NJ (1987).


# Dealloying Kinetics of $Cu_{1-x}Ti_x$ on $SiO_2$ Using *In Situ* X-Ray Diffraction


**S. W. Russell**[a]

*Department of Materials Science and Engineering, Cornell University, Ithaca, New York 14853*

**T. L. Alford**[b] **and J. W. Mayer***

[b]*Department of Chemical, Bio and Materials Engineering, and* [c]*Center for Solid State Science, Arizona State University, Tempe, Arizona 85287*



## ABSTRACT

We study the dealloying of Ti from $Cu_{1-x}Ti_x$ ($x \sim 10$ atom percent) alloy films on oxidized Si substrates in the temperature range of 375 to 490°C and an estimated $O_2$ partial pressure of $\sim 10^{-6}$ to $10^{-5}$ Torr. Reaction products were determined to be TiO and $Ti_2O_3$ and possibly $TiO_2$ at the free surface, and TiO at the $SiO_2$ interface, according to Rutherford backscattering spectrometry and Auger electron spectroscopy. We found that the Cu lattice parameter varies linearly with Ti concentration, and this variation is independent of temperature in this composition range. As a consequence, we were able to study the dealloying kinetics using *in situ* x-ray diffraction by monitoring the time dependence of the Cu lattice parameter. We observe that the reaction kinetics obey a parabolic rate law, *i.e.*, $X^2_{\mathrm{Ti,reacted}} = kt$, with a single activation energy of $1.6 \pm 0.1$ eV, suggesting that one process governs dealloying kinetics over this temperature range. In addition, we note a pronounced composition dependence, in that the reaction rate increases sharply with increasing Ti concentration. These observations suggest that Ti diffusion in Cu is the rate-limiting kinetic process for the dealloying reactions in this temperature regime. We model the dealloying reaction and in so doing estimate the diffusion coefficient for Ti in these alloy films.


## Introduction

Interest in copper metallization for very large scale integration (VLSI) in recent years has spawned numerous research endeavors. The advantages of using copper instead of aluminum for on-chip metallization schemes lie in its higher electrical conductivity and higher resistance to electromigration.[1,2] As with any developing materials system, much of the current research is directed toward circumventing the limitations of copper for this application through novel processing techniques. Two important obstacles to the introduction of copper for on-chip metallization are (*i*) the poor adhesion of copper to dielectric layers, such as $SiO_2$, and (*ii*) the high reactivity of copper, relative to aluminum, with oxygen in the ambient. Therefore, any fabrication scheme using copper as an on-chip interconnect must account for these materials limitations.

A novel approach proposed to address both of these problems simultaneously is to co-deposit Cu and another element, such as Ti [$\sim$10 atom percent (a/o)] onto $SiO_2$, then react in a nitriding ambient. Pure Ti reacts with $SiO_2$ to form $Ti_5Si_3$ and $TiO_W$ to an appreciable degree above $\sim$700°C [3] but may occur as low as 400°C. [4] The occurrence of this reaction at the alloy/$SiO_2$ interface promotes the adhesion of Cu to $SiO_2$ [5-7] and limits the drift of Cu into the oxide under bias thermal stress (BTS).[8,9]

In addition, Ti co-deposited with Cu reacts with nitriding agents such as $N_2$ at 800°C [10] to form a TiN layer on the alloy surface. Li *et al.* reacted alloy films in $NH_3$ instead of $N_2$ to reduce the nitridation temperature from 800 to


* Electrochemical Society Active Member.

[a] Present address: Department of Chemical, Bio and Materials Engineering, Arizona State University, Tempe, AZ 85287-6006.

550°C. [11] This process has been shown to form a nitride on the free surface that protects the underlying Cu from subsequent oxidation[12] as well as interdiffusion with Al. [13] The simultaneous segregation of Ti to all alloy interfaces effectively encapsulates the Cu, which simultaneously promotes adhesion, provides oxidation protection, and limits bias thermal stress one processing step, independent of the geometry of the Cu, *i.e.,* blanket film or patterned line.

Cu and Ti also form several intermetallic compounds that might be expected to precipitate in the composition range of these co-deposited alloy films, such as $Cu_3Ti$ and $Cu_4Ti$. [14,15] Forming these compounds degrades the electromigration resistance of the Cu relative to that of the alloy,[16] and in addition, would be expected to increase the line resistance by consuming Cu. Thus, the $SiO_2$ reduction at the lower interface and the nitridation reaction at the free surface must both compete with intermetallic compound formation within the alloy film.

The disadvantage of using alloys is that the presence of an alloying element greatly increases the electrical resistivity.[17] Ti was found to increase the resistivity of Cu linearly in co-evaporated alloys up to ~25 a/o Ti with a slope of ≈6.45 μΩ-cm/a/o Ti, yielding a value of 72 μΩ-cm at 10 a/o Ti. [18] To demonstrate feasibility as a manufacturable process, processing steps subsequent to deposition must insure that the final resistivity approaches that of pure Cu, 1.7 μΩ-cm. [19]

Other elements have been proposed as potential alloying elements for Cu in integrated circuit applications. Cu alloyed with 1 a/o Cr was found to have better adhesion to $SiO_2$ without sacrificing low resistivity,[20] although more than 15 a/o was required for better adhesion to $Al_2O_3$. [21] Ding *et al.* [22,23] demonstrated that the addition of Al or Mg to Cu via co-sputtering improves both adhesion to $SiO_2$ via an interfacial reaction and resistance to oxidation via formation of surface and interfacial oxides ($Al_2O_3$ or MgO), which act as diffusion barriers/adhesion promoters. Of these two elements, Mg appears the most promising because of postprocessing resistivity approaching 2 μΩ-cm, which is the same value obtained for as-sputtered Cu. Nevertheless, such oxide barriers may suffer due to their relatively high resistivity and high dielectric constant as compared to metal nitrides.

The simultaneous nitridation and interfacial reaction of $Cu_{1-x}Ti_x$ films is appealing from a processing point of view, but in a scientific sense, one would like to examine each reaction separately. This study investigates the reaction between $Cu_{1-x}Ti_x$ alloy films and an $SiO_2$ substrate. To minimize the competition between the substrate reaction and ambient reactions, reactions were performed in a nominal vacuum (~$10^{-5}$ Torr). However, the $O_2$ partial pressure in these systems remained high enough to cause some of the Ti to segregate to the free surface to form an oxide layer, and so these two separate reactions were monitored simultaneously.

Rutherford backscattering spectrometry (RBS) was used to determine the initial compositions and thicknesses of the as-deposited $Cu_{1-x}Ti_x$ alloy films and to quantify Ti segregation in reacted films. To perform additional compositional depth profiling, especially for low Z elements, we used Auger electron spectroscopy (AES) combined with ion sputtering. The chemical state of the various titanium oxide phases that formed at the free surface and at the $SiO_2$ interface were identified by the shape of the Ti Auger peak.

We found that the Cu lattice parameter varied linearly with Ti concentration over the temperature and compositional range of interest. Making use of this behavior, we investigated the kinetics of Ti dealloying by monitoring the position of the Cu (111) peak, and in so doing the Cu lattice parameter, as a function of time during *in situ* x-ray diffraction (XRD) at various temperatures.

Previous researchers have monitored the intensity of crystalline XRD peaks *in situ* to determine the kinetics of such solid-state processes as the crystallization of amorphous materials,[24] bulk crystalline-phase transformations,[25] precipitation from a supersaturated solid solution,[26] phase growth in diffusion couples,[27] surface oxidation,[28] and diffusion-induced grain boundary migration.[29] Few researchers have chosen to investigate the kinetics of a transformation by using *in situ* XRD to monitor the time evolution of the position of a particular peak. Köster *et al.* [30] studied α-Fe precipitation from $Fe_{73.4}Cu_1Nb_{3.1}Si_{13.4}B_{9.1}$ and correlated the α-Fe lattice parameter with Si concentration in the precipitates. They monitored how the Si concentration varied with the amount crystallized, which in itself was measured by the XRD peak linewidth.

The study most similar to that described in this paper was given by Biegel *et al.,* [31] who used the position of the diffraction peak of Nb supersaturated with Co to monitor the kinetics of Co dealloying to form an amorphous phase. In this study, the angular position of the NbCo (110) peak varied as $t^{1/2}$. By a Taylor expansion of Bragg's law, $\lambda = 2d \sin\theta$, one can show that the $d$-spacing varies linearly with $2\Theta$ over a small angular range, *i.e.,* $d \approx d_o - (\lambda \cos\theta_o/\sin^2\theta_o)(2\theta - 2\theta_o)$ with $d_o \equiv d$ at $2\theta = 2\theta_o$. Therefore, this observed kinetic dependence coupled with a linear variation in the Nb lattice parameter with increasing Co content indicates diffusion-controlled growth of the amorphous phase.

Two possibilities exist to drive Ti dealloying from $Cu_{1-x}Ti_x$ alloy films. These are (*i*) the precipitation of intermetallics within the bulk of the film, and (*ii*) the reaction of Ti at the free surface and at the $SiO_2$ interface to form Ti oxides such as $Ti_2O$, α-TiO, γ-$Ti_3O_5$, $Ti_2O_3$, or $TiO_2$. We show that titanium oxide formation dominates over the temperature range 375 to 490°C, with Ti diffusion out of the Cu alloy matrix being the rate-limiting kinetic process. A simple model describing the reaction kinetics is developed to estimate the Ti diffusion coefficient in these films.

## Experimental

Alloy films of $Cu_{1-x}Ti_x$ were co-deposited by electron beam evaporation with a base pressure of ~$5 \times 10^{-8}$ Torr onto oxidized Si (100) substrates, with an $SiO_2$ thickness of ≈7000 Å. The pressure rose to ~$1 \times 10^{-6}$ Torr during the evaporation. Deposited and reacted film composition profiles were measured with RBS using a General Ionex 1 MV tandetron accelerator with a 2.8 MeV $He^{2+}$ beam at a 7° tilt angle, and by AES using a Perkin-Elmer 590 Auger electron spectrometer with a 1 keV $Ar^+$ ion gun for sputtering and a 5 keV primary electron beam. The energy windows for elemental profiling were 401 to 423 eV for the Ti LMV Auger peak, 490 to 517 eV for O KLL, 900 to 925 eV for Cu LMM, and 1592 to 1626 eV for Si KLL. The Auger profile was used in conjunction with RBS to quantify the layer compositions; the shape of the Ti LMV Auger peak was used to determine the chemical state of Ti in the various layers.

Dealloying kinetics were performed by monitoring the shift in the position of the Cu (111) peak during *in situ* XRD in Θ-Θ mode using Cu Kα radiation (λ = 1.5418 Å) on a vacuum ($5 \times 10^{-6}$ to $5 \times 10^{-5}$ Torr) hot stage mounted on a Scintag I diffractometer. The (111) peak was chosen because of its intensity due to the high degree of (111) texturing in these films. Samples were mounted onto a $Pt_{60}Rh_{40}$ strip and affixed with silver paint to insure good thermal contact. Samples were heated by passing an electrical current through this strip. The temperature was independently monitored by a $Pt/Pt_{90}Rh_{10}$ thermocouple mounted on the other side of the heating strip from the sample. A feedback loop was employed to precisely control the temperature, and a vacuum of ~$5 \times 10^{-5}$ Torr was maintained during anneals.

## Results

*Elemental profiling using RBS and AES.*—A schematic diagram of the sample configuration both before and after the dealloying reaction is shown in Fig. 1 and may be used for reference throughout this paper. Figure 2 is an RBS spectrum of an as-deposited film. This spectrum identifies the film as $Cu_{90}Ti_{10}$ of thickness 2350 Å. The kinetics of this particular film was subsequently studied using *in situ* XRD. Spectra of films after annealing are shown in Fig. 3.

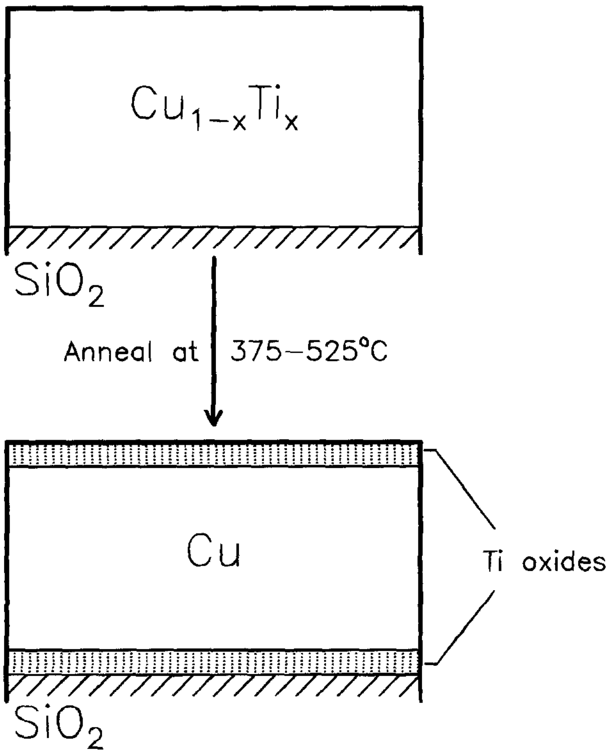


**Fig. 1. Schematic diagram depicting the reaction of co-deposited $Cu_{1-x}Ti_x$ films on $SiO_2$ substrates in a slightly oxidizing ambient.**

After annealing the sample at 375°C for 12 h, little apparent change is resolvable in the RBS spectrum as compared to that of the as-deposited film, although appreciable Ti segregation to both the $Cu/SiO_2$ interface and to the free surface can be seen after annealing for 2 h at both 440 and 525°C. A slight surface segregation of Ti in each annealed sample is observed, as is the appearance of a small O surface peak, suggesting that some Ti oxide phase formed at the surface. The sample annealed at 525°C for 2 h is shown with an overlayed simulation in Fig. 4. The thickness of the surface Ti-O layer as estimated by RBS is 375 Å and the composition of this layer was found to be in the range TiO-$TiO_2$. The layer formed between the Cu and the $SiO_2$ substrate was estimated to have a thickness of ~200 Å and a composition of ~$TiOSi_{0.5}$.

AES profiles of these three samples are given in Fig. 5-7. Several features are readily apparent from these profiles.

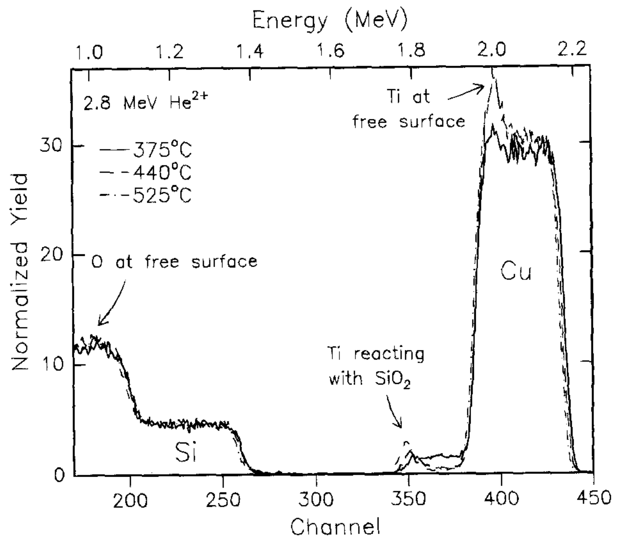


**Fig. 3. RBS spectra of $Cu_{90}Ti_{10}$ after annealing at 375, 440, and 525°C.**

The Si and O concentrations in the as-deposited film (Fig. 5) are nearly zero; these signals are well within the experimental noise levels. No Ti segregation to either interface is observed. The discontinuity at the $Cu/SiO_2$ interface is a result of charging that occurs as the insulating oxide is exposed by $Ar^+$ ion sputtering. We estimate the sputtering rate through the alloy film as approximately 2350 Å/75 min, or 300 Å/min, by comparing the AES depth profile with the RBS spectrum.

Anneals of 375°C for 12 h results in some segregation of Ti to the free surface and a corresponding increase in O, suggesting that a surface Ti-O layer has formed (Fig. 6). An increase in the Cu intensity adjacent to both interfaces is suggestive of an increase in Cu concentration due to Ti dealloying, although a Ti-rich interfacial layer is not observed at this temperature, possibly due to charging effects. We use the AES intensities of Ti and O from the $TiO_W$ layer formed by annealing pure Ti on $SiO_2$ as a calibration[3] and RBS to determine the actual compositions. Assuming $C_O/C_{Ti} = k(I_O/I_{Ti})$, with $k$ constant, we find $k = 0.82$ to 0.83. Beam parameters are identical to those of the calibration experiment, and so this value for $k$ is used to determine the composition of the surface layer which formed on $Cu_{1-x}Ti_x$ alloy films as ~$TiO_{1.6}$-$TiO_{1.7}$. No penetration of either O or Si into the film is observed. Ti-depleted regions exist below

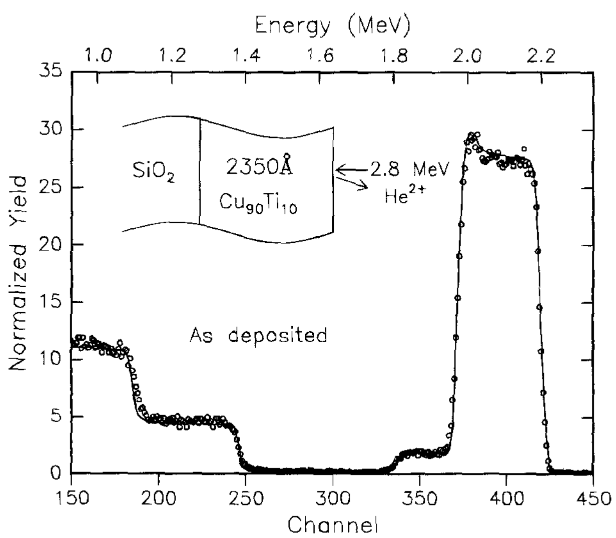


**Fig. 2. RBS spectrum of the as-deposited $Cu_{1-x}Ti_x$ film with simulation overlayed. Incident beam energy 2.8 MeV $He^{2+}$; tilt angle 7°.**

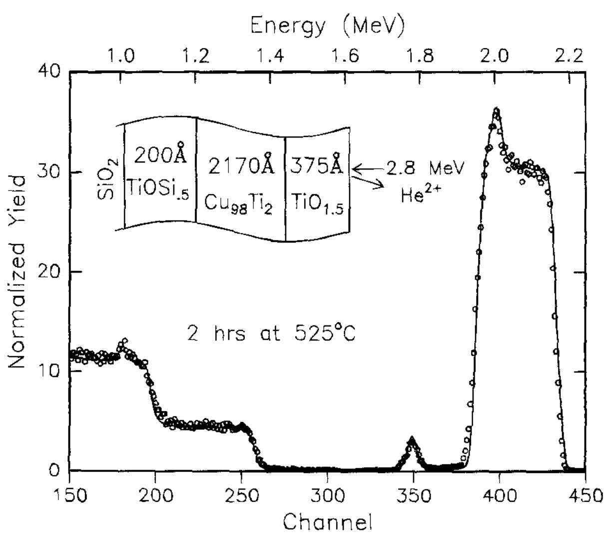


**Fig. 4. RBS spectrum of $Cu_{90}Ti_{10}$ annealed 2 h at 525°C with simulation overlayed.**

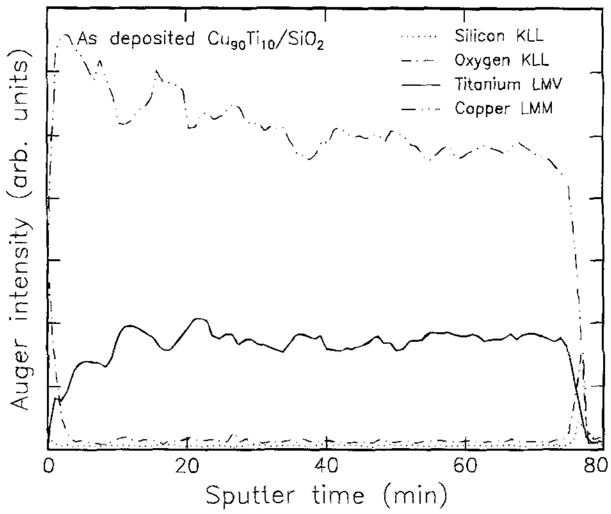


**Fig. 5. AES depth profile of as-deposited $Cu_{90}Ti_{10}$ film, with Cu (LMM), Ti (LMV), Si (KLL), and O (KLL) signals plotted.**

the surface oxide layer and adjacent to the $SiO_2$, but between these depleted zones is an area of roughly constant composition. The peak Ti concentration in the $Cu_{1-x}Ti_x$ layer is ~7 a/o lower than that of the as-deposited film. Charging is observed at the $Cu/SiO_2$ interface as a discontinuity in all Auger signals.

Annealing at 525°C results in complete segregation of Ti to both the free surface and the $Cu/SiO_2$ interface (Fig. 7). The near-surface Ti-oxide layer varies in composition from TiO to $TiO_{1.5}$, and the Ti-oxide layer at the $Cu/SiO_2$ interface varies in composition from $TiO_{0.8}$-TiO. The residual Ti content in the Cu layer is ~0.8 a/o. All results are in good agreement with RBS.

*Chemical analysis by Auger peak shape.*—Information about the chemical environment of the various elements in these films can be obtained from the Auger spectra in select regions of each sample, in comparison to the known spectra of previously investigated compounds, such as the titanium oxides. Figures 8-10 are the differential Ti LMV Auger spectra for $Cu_{90}Ti_{10}$ on $SiO_2$ as deposited, 12 h anneal at 375°C, and 2 h anneal at 525°C, respectively. The Ti LMV peak is shown since it exhibits the most pronounced changes from layer to layer, the Cu LMM peak remains nearly unchanged in position and shape throughout these heat-treatments. These peaks are sensitive to metal-oxygen bonding and can suggest which oxide phases have formed.

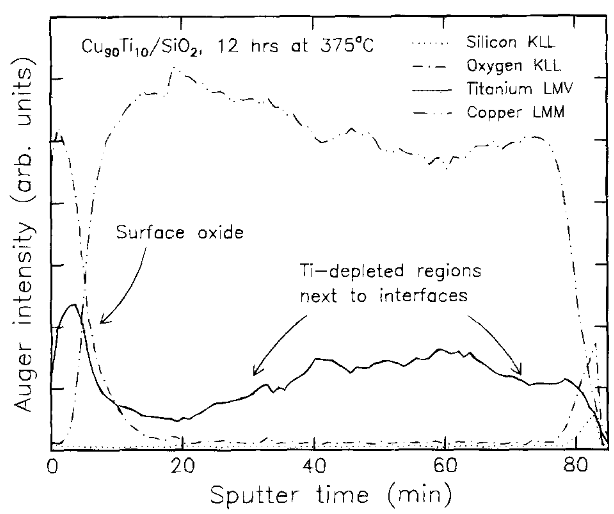


**Fig. 6. AES depth profile of $Cu_{90}Ti_{10}$ after annealing 12 h at 375°C depicting formation of Ti oxide at the free surface and depletion of Ti adjacent to each interface.**

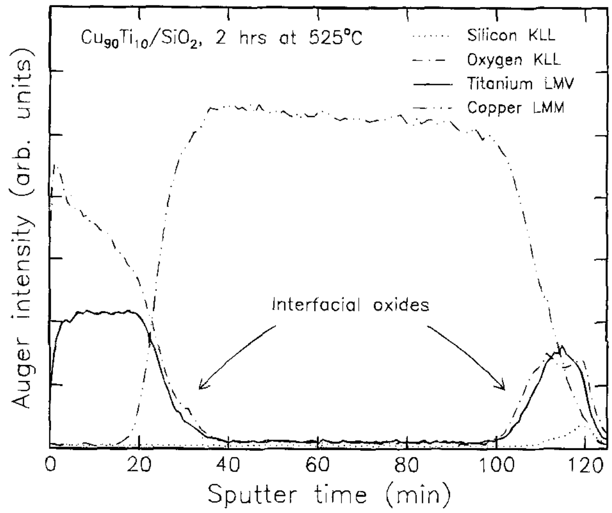


**Fig. 7. AES depth profile of $Cu_{90}Ti_{10}$ after annealing 2 h at 525°C depicting formation of Ti oxides at the free surface and adjacent to the $SiO_2$. Ti has been almost completely removed from the alloy.**

The LMV peak for the as-deposited film (Fig. 8) is at ~416.5 eV (the position corresponds to the minimum in the differential spectra, as per convention), which is near the expected position for metallic Ti. Despite the dissolution of Ti in the face-centered cubic (fcc) Cu lattice, there is little change in this Auger peak. The general characteristics of the peak shape are expected for the LMV transition of pure Ti.[32]

The spectrum from the 375°C anneal is characterized by several distinct regions, as seen in the depth profile of Fig. 6. The Ti LMV peak from the near-surface oxide layer (Fig. 9a) has a shoulder on its low energy side at 406 eV. The shoulder is at nearly the same height as the main peak, itself shifted by ~0.5 eV relative to that of Ti in the as-deposited $Cu_{90}Ti_{10}$. The peak corresponding to the remaining $Cu_{1-x}Ti_x$ (Fig. 9b) is featureless and of the expected shape for metallic Ti.

Figure 10 shows spectra from two regions: (a) the near-surface oxide layer and (b) the oxide layer adjacent to $SiO_2$. A chemical change has occurred in the near-surface layer (Fig. 10a) due to the extended heat-treatment. The LMV peak is broad with a low energy shoulder at 406 eV, similar to that of Fig. 9a, with the main peak shifted by almost the same amount (~0.5 eV) relative to that of the as-deposited Ti. However, at 525°C the low energy shoulder is higher than the main peak, whereas at 375°C, the main peak is

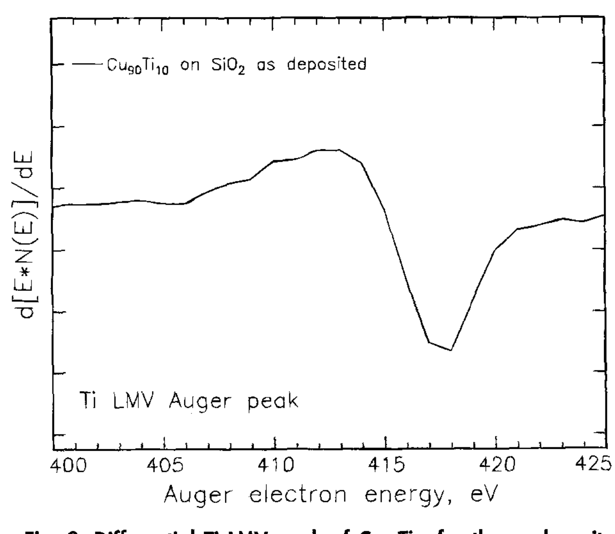


**Fig. 8. Differential Ti LMV peak of $Cu_{90}Ti_{10}$ for the as-deposited $Cu_{90}Ti_{10}$ film. Shape and position are those expected for metallic Ti.**

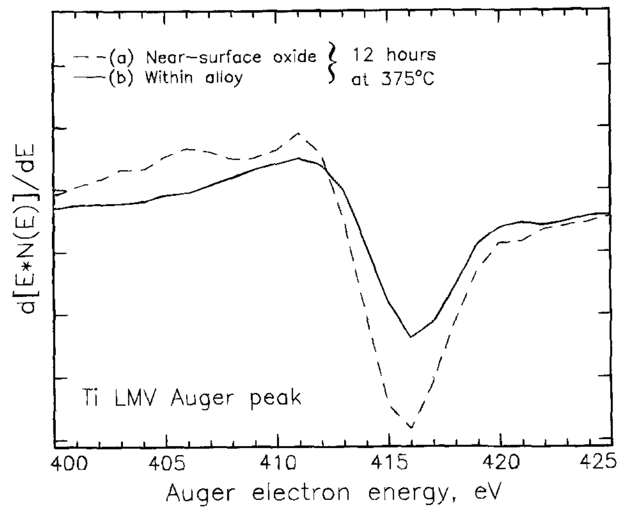


**Fig. 9. Differential Ti LMV peak of $Cu_{90}Ti_{10}$ after annealing 12 h at 375°C (a) from the near-surface oxide, (b) from the underlying alloy.**

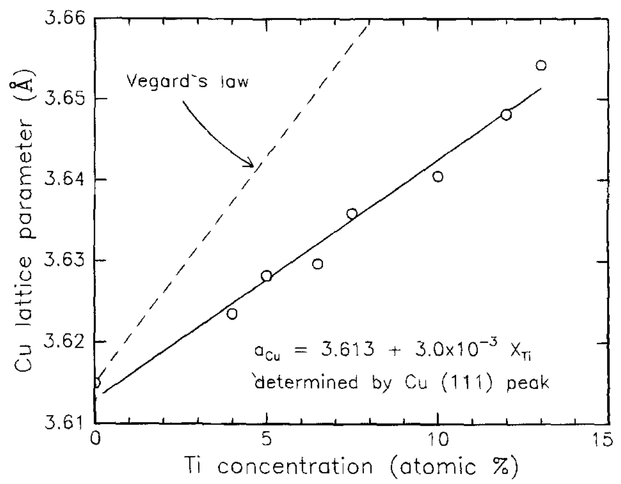


**Fig. 11. Variation of Cu lattice parameter with Ti concentration at room temperature, according to Eq. 1, found by fitting a Lorentzian to the Cu (111) XRD peak using Cu-K$\alpha$ radiation ($\lambda$ = 1.5418 Å).**

greater. The LMV peak from Ti accumulating at the Cu/$SiO_2$ interface (Fig. 10b) exhibits an asymmetric shape, unshifted relative to the as-deposited Ti. Although the appearance of a low energy shoulder near ~406 eV is apparent, this shoulder is much smaller than those corresponding to Ti in the near-surface oxide formed after 375°C (Fig. 9a) or 525°C (Fig. 10a) anneals.

These spectra indicate the chemical environment of Ti in the various layers since the Ti LMV peak (416 eV) is sensitive to the presence of oxygen.[33] For TiO, the Ti LMV peak exhibits a low energy shoulder at ~407 eV, while the primary peak is shifted by ~1 eV to higher energies relative to metallic Ti. For $TiO_2$, the LMV peak broadens and shifts to lower energies by ~2 eV. $Ti_2O_3$ exhibits characteristics of both TiO and $TiO_2$ in that the LMV peak forms a low energy shoulder, but the shoulder is closer in height to the main peak than that found in TiO. These results indicate that TiO and/or $Ti_2O_3$ form at the free surface at 375°C and have grown thicker by 525°C, with perhaps $TiO_2$ forming as well. At the Cu/$SiO_2$ interface, the chemical state of Ti is what is expected for TiO. The Ti remaining in the $Cu_{1-x}Ti_x$ layer remains in a similar chemical state to that of the as-deposited Ti, as it does not exhibit any of the distinctive peak shape changes characteristic of Ti oxidation.

*Cu lattice parameter as a function of Ti concentration and temperature.*—An expansion of the fcc Cu lattice was observed due to Ti incorporation upon co-evaporation. We performed a series of co-depositions ($X_{Ti}$ = 0, 4, 5, 6.5, 7.5, 10, 12, and 13 a/o, as measured by RBS) to determine the variation in the Cu lattice parameter with Ti concentration. The lattice parameter was found by a Lorentzian fit to the Cu (111) XRD peak after a linear background subtraction; *i.e.*, $I(2\Theta) = I(2\Theta_B) \times w^2/[w^2 + (2\Theta - 2\Theta_B)^2]$, where $I(2\Theta_B)$ is the maximum intensity at the Bragg angle $2\Theta_B$, and $w$ is the full-width at half-maximum. We then calculate the $d$-spacing from Bragg's law, $\lambda = 2d \sin \Theta$, and the lattice parameter from $a_{Cu} = \sqrt{3}d_{111}$. A linear relationship between $a_{Cu}$ and $X_{Ti}$ held over this composition range, but at higher concentrations the as-deposited films were found to be amorphous. This relationship is expressed as

$$a_{Cu} = a_o + \delta X_{Ti} \quad [1]$$

with $\delta \equiv da_{Cu}/dX_{Ti}$. This relation is plotted in Fig. 11, with $a_{Cu}$ = 3.613 Å (3.615 Å from ASTM card 4-836) and $\delta = 3.0 \times 10^{-3}$ for $X_{Ti}$ in a/o. This linearity was observed to hold up to the Ti concentration at which an identifiable (111) peak was no longer observed, ~15 a/o. Using the value $a$ = 2.950 Å for HCP $\alpha$-Ti (ASTM card 5-682) to define the size of the Ti atom, an fcc lattice of Ti would have $a_{Ti}$ = 4.172 Å. Vegard's law for the Cu-Ti system can be expressed as $a_{Cu} = 3.615 + 0.00557X_{Ti}$ in Å for $X_{Ti}$ in a/o. The measured value of $\delta$ is ~43% smaller than that predicted by Vegard's law. Thermodynamically, this implies a negative deviation from ideality in the $Cu_{1-x}Ti_x$ solid solution, consistent with the presence of intermetallic compounds in this system.

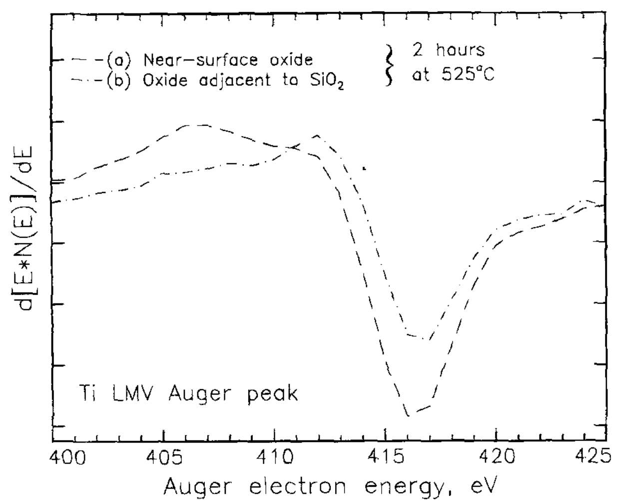


**Fig. 10. Differential Ti LMV peak after annealing 2 h at 525°C (a) from the near-surface oxide, (b) from the oxide adjacent to $SiO_2$.**

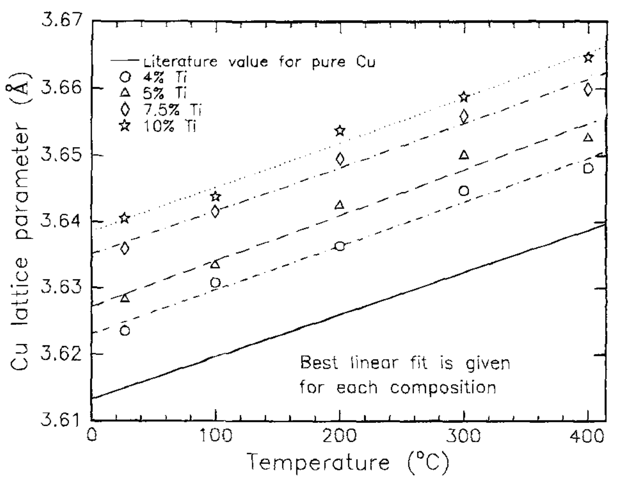


**Fig. 12. Variation of Cu lattice parameter with temperature according to Eq. 2 for 4, 5, 7.5, 10 a/o Ti in Cu. Solid line is the expected value for pure Cu.**

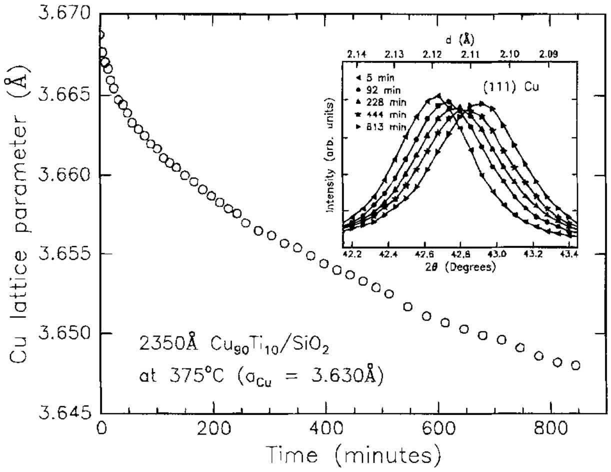


**Fig. 13. Time evolution of the Cu lattice parameter at 375°C, found by fitting a Lorentzian to the Cu (111) peaks using *in situ* XRD. Shown in the insert are selected XRD scans at 5, 92, 228, 444, and 813 min after reaching the final anneal temperature.**

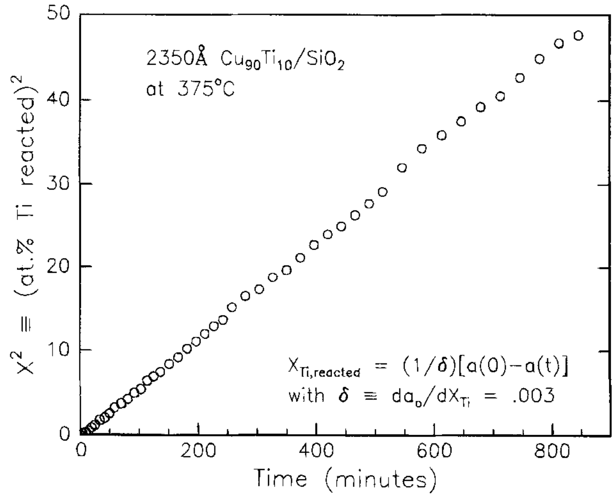


**Fig. 14. Square of the amount of Ti reacted (a/o) as a function of time at 375°C. The slope of this line is the reaction rate $k_x$ defined in Eq. 5.**

To quantify the $Cu_{1-x}Ti_x$ composition at all temperatures, we must relate $a_{Cu}$ to $T$ for different compositions. For pure Cu, $a_{Cu}$ varies linearly with temperature

$$a_{Cu} = a_o(1 + \alpha_{Cu}\Delta T) \qquad [2]$$

where $\alpha_{Cu} \equiv (1/a_{Cu})(da_{Cu}/dT)$ is the thermal expansion coefficient, $\approx 17.6 \times 10^{-6}$/°C.[34] If $\alpha_{Cu}$ varies with Ti concentration, then the expansion due to Ti incorporation, δ, will also vary with temperature, making subsequent analysis more difficult.

Co-deposited alloy films of four different Ti concentrations are monitored *in situ* by XRD, following the evolution of the Cu (111) peak at temperatures of 27, 100, 200, 300, and 400°C. In Fig. 12, $a_{Cu}$ is given as a function of temperature for these four concentrations. The fitted values of $\alpha_{Cu}$ for samples of 4, 5, 7.5, and 10 a/o Ti are 18.4, 19.1, 18.1, and $18.4 \times 10^{-6}$/°C, respectively. The literature value for $a_{Cu}(T)$ for pure Cu is also plotted for comparison; our measured values for $\alpha_{Cu}$ are within 5% of that value. Above 400°C, Ti dealloying becomes important in the time scale required for this measurement, and therefore we could no longer assume that all of the originally deposited Ti remains dissolved in the fcc Cu phase.

*Dealloying kinetics of $Cu_{90}Ti_{10}/SiO_2$ by in situ x-ray diffraction.*—As we observe that the Cu lattice parameter varies linearly with Ti concentration over the temperature range of interest (Eq. 1), we may in turn calculate the composition of the fcc Cu phase by measuring the lattice parameter. This approach assumes that only Cu and Ti are constituent elements, which the Auger and RBS results indicate. Using *in situ* x-ray diffraction, we monitor the time evolution of the Cu (111) peak at 375, 400, 420, 435, 440, 455, 470, 480, and 490°C. Sample temperatures were ramped from room temperature to the final annealing temperature at a rate of 100°C/min. The "zero time" for annealing was taken as the time at which the final temperature was reached. Spectra of this peak taken at successive times at 375°C are shown in the insert in Fig. 13. The dominant feature is a shifting of this peak to higher angles, *i.e.*, smaller $d$-spacings. By fitting a Lorentzian to each peak, we determine the peak position within 0.002-0.003° 2Θ. This corresponds to an accuracy in $d$-spacing of $(\lambda/4)(\cos\Theta/\sin^2\Theta)\Delta(2\Theta)$, or ±0.0005 to 0.0008 Å for $\Theta = 21.7°$ and $\lambda = 1.5418$ Å. The five peaks shown, taken after 5, 92, 228, 444, and 813 min at 375°C, correspond to positions of $2\Theta$ = 42.66, 42.73, 42.78, 42.83, and 42.90°, implying an average Cu lattice parameter of $a(t)$ = 3.6676, 3.6620, 3.6579, 3.6537, and 3.6482 Å, respectively. The time evolution of the Cu lattice parameter at 375°C is plotted in Fig. 13.

Using the linear relationship between the Cu lattice parameter and the Ti concentration (Eq. 1), we can easily relate $a_{Cu}$ to the amount of (unreacted) Ti remaining in the fcc Cu phase. With $a(0)$ = 3.6687 Å to 10 a/o Ti at this temperature, the amount of Ti remaining in the Cu is calculated as 9.7, 7.9, 6.6, 5.2, and 3.5 a/o at these anneal times.

An absolute error in the x-ray peak position resulting from any misalignment of the heating stage may occur, and we must account for this possibility. To do this, we take the difference between the measured initial value of the lattice parameter $a(0)$ and the instantaneous value $a(t)$. This difference was used in all calculations rather than the difference between $a(t)$ and $a_{Cu}$ [$\equiv a(\infty)$], and by treating data in this manner rather than via Eq. 1, we eliminate this error. As a result, the amount of Ti that has reacted is calculated directly. In units of a/o, the amount of reacted Ti, $X_{Ti,reacted}$, is given by

$$X_{Ti,reacted}(t) = \frac{a(0) - a(t)}{\delta} \qquad [4]$$

where $a(0)$ and $a(t)$ are the initial and instantaneous lattice parameters of Cu, respectively, and $\delta = da_{Cu}/dX_{Ti}$. The lattice parameters above correspond to 0.3, 2.1, 3.4, 4.8, and 6.5 a/o Ti reacted.

If we plot the square of $X_{Ti,reacted}(t)$ *vs.* $t$, linear behavior is observed, indicating that the dealloying process obeys a parabolic rate law

$$X^2_{Ti,reacted} = k_x t \qquad [5]$$

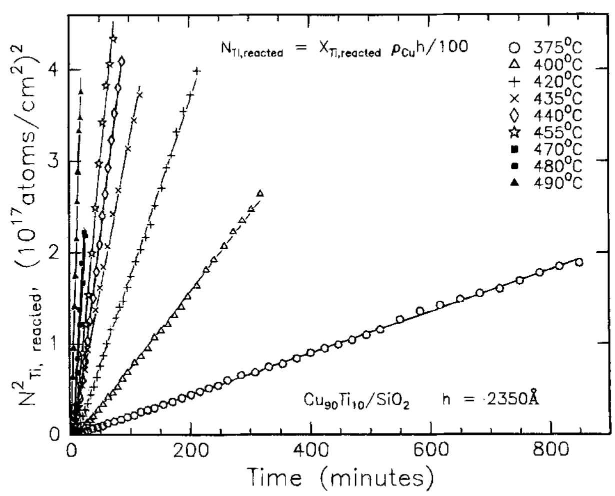


**Fig. 15. Square of the amount of Ti reacted (atom/cm²) as a function of time at 375 to 490°C. The slopes of these lines are the reaction rates $k_N$ [(atom/cm²)²/s]. $k_N \equiv k_x\rho_{Cu}h/100$.**

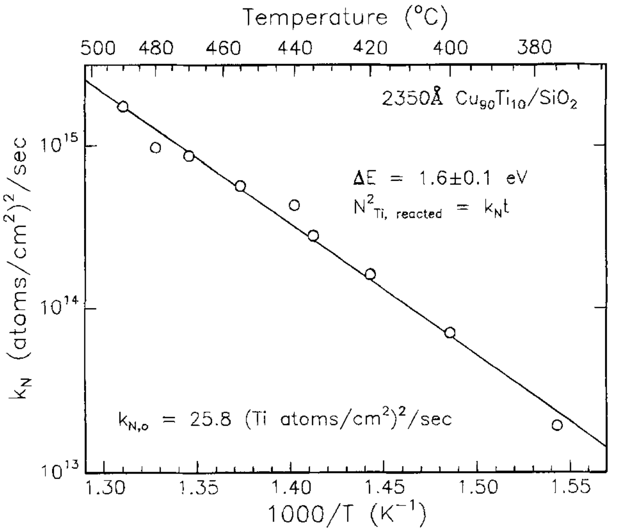


**Fig. 16. Arrhenius plot of the reaction rates $k_N$ at $375 \leq T \leq 490$°C.**

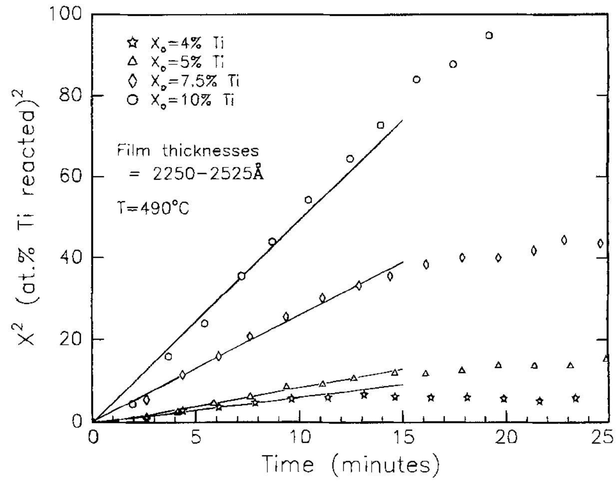


**Fig. 17. Square of the amount of Ti reacted (a/o) as a function of time at 490°C for four different initial Ti concentrations.**

This is plotted in Fig. 14 during a 375°C anneal. A kinetic expression such as this implies that diffusion-controlled layer growth is likely to be the rate-limiting process governing the dealloying reaction.

We can relate the a/o Ti reacted to the number of reacted Ti atoms per unit area of the film, $N_{\text{Ti,reacted}}$ (atom/cm$^2$) by knowing the film thickness, $h$, and the film density, $\rho$. The film thickness is 2350 Å according to RBS; the film density is close to that of pure Cu, $\rho_{\text{Cu}} = 8.47 \times 10^{22}$ atom/cm$^2$. This number is calculated using the relationship $N_{\text{Ti,reacted}} = (X_{\text{Ti,reacted}}/100)\rho_{\text{Cu}}h$. Therefore, the dealloying rate may also be given by $N^2_{\text{Ti,reacted}}(t) = k_N t$. This relationship is plotted in Fig. 15 at each reaction temperature. Only anneals at temperatures from 375 to 490°C were used in the kinetic study; above 490°C, the dealloying reaction occurs too rapidly to be monitored accurately in real time using *in situ* XRD. From the Arrhenius plot given in Fig. 16, we extract an activation energy of $\Delta E = 1.6 \pm 0.1$ eV for the dealloying reaction and an exponential prefactor $k_{\text{N,o}}$ equals 25.8 (Ti atom/cm$^2$)$^2$/s, assuming $k_N = k_{\text{N,o}} \exp(-\Delta E/k_B T)$, with $k_B$ = Boltzmann's constant.

*Composition dependence of dealloying kinetics.*—Dealloying kinetics were found to depend strongly on the initial film composition, with films initially richer in Ti possessing more rapid reaction rates. Four films, similar in thickness but of initially different compositions, were annealed at 490°C with *in situ* XRD to monitor dealloying kinetics. The compositions chosen were 4.0, 5.0, 7.5, and 10.0 a/o Ti and film thicknesses were 2250, 2350, 2525, and 2350 Å, respectively. In Fig. 17, we plot $X^2_{\text{Ti,reacted}}$ *vs.* time for each composition; straight lines represent linear fits to the initial stages of dealloying. Note that a departure from parabolic kinetics occurs at shorter times for films containing initially less Ti. With $X^2_{\text{Ti,reacted}} = k_x t$, the measured values of $k_x$ are 0.60, 0.86, 2.5, and 4.9 (a/o Ti)$^2$/min at 490°C, respectively. In other words, a two and one-half-fold increase in $X_o$ results in more than an eightfold increase in $k_x$. These samples were also used to determine the composition dependence of the thermal expansion coefficient (Fig. 12). The composition dependence of $k_x$ is plotted in Fig. 18. A cubic equation was found to exhibit the best fit, as may be explained by our model below.

## Discussion

*Driving forces for titanium dealloying.*—Several possible physical driving forces exist for titanium dealloying. Ti and Cu form a series of intermetallic compounds according to the phase diagram, as discussed previously in this paper. Since the stoichiometries of these compounds are more Ti-rich than that of the as-deposited $Cu_{1-x}Ti_x$ alloy film, precipitation of any of these compounds would lead to a net removal of Ti from the Cu lattice. In addition, Ti forms several oxides by reacting with both ambient oxygen and with $SiO_2$. With an operating total pressure in the range $5 \times 10^{-6}$ to $5 \times 10^{-5}$ Torr, it is likely that annealing occurs well above the equilibrium $O_2$ partial pressure for the known Ti-O reactions, which is $\sim 3.5 \times 10^{-53}$ atm ($3 \times 10^{-50}$ Torr) for $TiO_2$ formation at 500°C.[35] Lastly, the Ti in the as-deposited $Cu_{1-x}Ti_x$ alloy is supersaturated; the solubility of Ti in Cu is small due to their dissimilar lattice structures, varying from ~0.8 a/o at 500°C to a maximum of ~8.0 a/o at 800°C.[14] The resulting lattice expansion due to Ti incorporation in the Cu lattice produces an elastic strain energy proportional to $(\Delta a/a_o)^2$. For 10 a/o Ti in Cu, $\Delta a/a_o = 0.0088$ at room temperature. Given that Young's modulus for Cu is 110 GPa,[36] the strain energy per unit volume is 3.8 J/cm$^3$, which is 26.9 J/mol. This number must be compared to the relevant free energies of oxide formation in this system. For the oxidation of Ti, $\Delta G^\circ_f$ equals −474 kJ/mol for α-TiO, −1320 kJ/mol for $Ti_2O_3$ and −2033 kJ/mol for $Ti_3O_5$ at $T$ = 427°C,[37] all of which are orders of magnitude larger than the strain energy. It is therefore likely that the driving force for Ti dealloying is chemical in nature.

The appearance of Ti-O bonding at both interfaces in the annealed samples, as evidenced by Auger peak shape and by both RBS and Auger depth profiling, suggests that Ti segregates to each interface due to the presence of oxygen and/or silicon. At the $Cu_{1-x}Ti_x/SiO_2$ interface, both Si and O are likely to be contributing to the driving force for Ti segregation; at the free surface, only O from the ambient

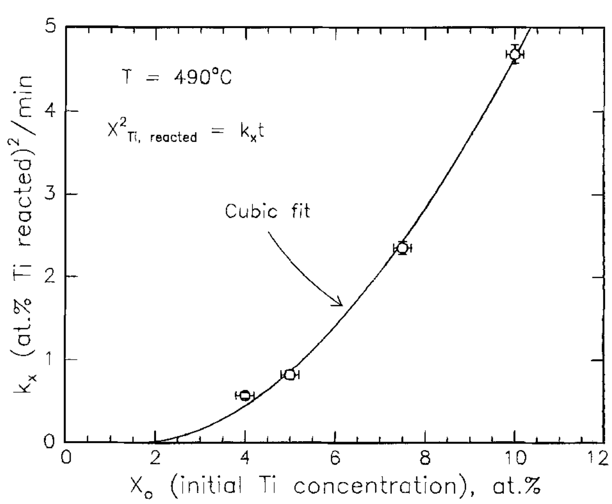


**Fig. 18. Concentration dependence of the reaction rate $k_x$ at 490°C.**

contributes. From our previous knowledge of the $Ti/SiO_2$ system,[3] we infer that such a double layer might indicate the formation of both Ti-Si and Ti-O layers from decomposition of $SiO_2$.

The temperature at which the alloyed Ti begins to reduce $SiO_2$ as found in this study (375°C) is approximately that observed for the onset of the pure $Ti/SiO_2$ reaction.[38] However, the geometry of the reaction zone is distinctly different for the alloy films in this study than for the pure metal, in which the Ti which has not been consumed by silicide formation acts as a sink for O atoms liberated by the $SiO_2$ reduction. The Ti lattice fills uniformly with interstitial O, eventually forming the α-TiO phase; this has been shown to result in nonparabolic Ti silicide formation kinetics.[3,39] By contrast, in the alloy geometry, no Ti lattice exists into which the O must diffuse for the reaction to proceed. The composition of the TiO phase which forms is probably constant during the course of the reaction as a result, and our Auger results seem to verify this.

*Rate-limiting kinetic process for titanium dealloying.*—A parabolic time dependence for the amount of dealloyed titanium suggests that diffusion is the rate-limiting kinetic process, either across the growing Ti oxide phases or out of the $Cu_{1-x}Ti_x$ alloy. The former scenario results in parabolic reaction kinetics since the oxide growth rate $dR_{\text{oxide}}/dt$ ($R_{\text{oxide}} \equiv$ oxide thickness) is proportional to the flux across the oxide, which in turn varies as $1/R_{\text{oxide}}$. This leads upon integration to a rate law of the form $R^2_{\text{oxide}} = kt$. The latter scenario results in parabolic reaction kinetics since as the oxide layer grows, it depletes a region in the underlying alloy film of Ti, and Ti atoms must diffuse across this depleted zone to sustain further growth. As the width of this region increases as $R_{\text{oxide}}$ with continued oxide growth, we again expect a rate law of the form $R^2_{\text{oxide}} = kt$. In either case, the kinetics are determined by diffusion over a distance that widens as growth continues, leading to parabolic growth. A parabolic rate law cannot distinguish between these two growth modes.

From our experiments, we ought to be able to determine which of these modes operates in the $Cu_{1-x}Ti_x/SiO_2$ system. Two of our experiments strongly indicate that diffusion of Ti out of the alloy film is the rate-limiting process. First, the existence of a concentration gradient in a particular phase in a thin film system suggests that diffusion across this phase may be slow relative to other processes. The Auger depth profile of the sample annealed at 375°C (Fig. 6) shows a distinct concentration gradient in the alloy film underneath the growing oxide layer. If diffusion across the oxide were slow relative to diffusion out of the alloy, we would expect the Ti profile within the alloy to remain uniform but decrease steadily with time, rather than exhibit a concentration gradient. Second, a dependence of the growth rate on Ti concentration is unlikely if diffusion across the oxide is rate limiting, but is necessary if diffusion within the alloy is rate limiting. The lower the concentration of Ti in the alloy film, the greater the width of the depletion zone within the film for the same amount of oxide formed. The greater the zone width, the slower the oxide growth rate, since the Ti atoms supplying oxide growth must diffuse a greater distance. The reaction rate at 490°C increases by a factor of 8.25 as the concentration of Ti in $Cu_{1-x}Ti_x$ increases from 4 to 10 a/o, as shown in Fig. 18. It is likely that an increase in this magnitude is due to the decreased distance across which Ti in the alloy must diffuse for more Ti-rich alloys to oxidize.

*Modeling the kinetics of Ti dealloying.*—If Ti diffusion within the alloy is the rate-limiting step, then we should be able to estimate the diffusion coefficient of Ti in Cu given the measured rate constants. To accomplish this, the following assumptions are made to simplify analysis: (*i*) the oxides at each interface have identical compositions and densities, begin growing at the same time and are growing at the same rate; (*ii*) the Ti profile in the alloy adjacent to each interface is linear, with the concentration equal to a constant (equilibrium) value adjacent to the oxide interfaces, and is equal to its initial concentration within the bulk of the alloy; (*iii*) the diffusion coefficient of Ti in the alloy is composition-independent; and (*iv*) diffusion across each oxide layer is rapid relative to diffusion within the alloy.

First, we must relate the amount of reacted Ti to a thickness of oxide grown. The amount of reacted Ti per unit area must be accounted for by the growth of a reaction product. If an oxide of thickness $R_{\text{oxide}}$, atomic density $\rho_{\text{oxide}}$, and a/o $X_{\text{oxide}}$ forms at each interface, then the number of Ti atoms that have reacted per unit area must be given by

$$N_{\text{Ti,reacted}} = 2R_{\text{oxide}} \frac{X_{\text{oxide}}\rho_{\text{oxide}} - X_o\rho_{\text{Cu}}}{100} \quad [7]$$

where $X_o$ is the initial amount (a/o) of Ti in the alloy, $\rho_{\text{Cu}}$ is the atomic density of Cu (assumed constant), and the factor of two reflects the fact that two oxides are growing simultaneously. Using the relationship between $X_{\text{Ti,reacted}}$ and $N_{\text{Ti,reacted}}$, and defining $b$ as the ratio of the atomic density of the oxide to that of Cu ($b \equiv \rho_{\text{oxide}}/\rho_{\text{Cu}}$), we obtain

$$R_{\text{oxide}} = \frac{X_{\text{Ti,reacted}}h}{2(bX_{\text{oxide}} - X_o)} \quad [8]$$

$X_{\text{Ti,reacted}}$ varies parabolically with time, *i.e.*, $X^2_{\text{Ti,reacted}} = k_x t$, with $k_x$ the parabolic growth rate in units of $(\text{a/o})^2$/s. From Eq. 6, we determine that the corresponding oxide thickness growth rate $k_R$ is related to $k_x$ according to

$$k_R = \frac{k_x h^2}{4(bX_{\text{oxide}} - X_o)^2} \quad [9]$$

The growth rate of the oxide, $dR_{\text{oxide}}/dt$, is proportional to the diffusional flux of Ti arriving at the interface, *i.e.*, $(C_{\text{oxide}} - C_E)dR_{\text{oxide}}/dt = D(\partial C/\partial r)|_{\text{interface}}$, with $D$ the chemical diffusion coefficient of Ti in Cu, $C_{\text{oxide}}$ the concentration of Ti in the oxide phase, and $C_E$ the (equilibrium) concentration of Ti in the alloy at the interface. The concentration of an element j in phase i is $\rho_i X_{ji}$, and so we recast the growth rate in terms of atomic fractions

$$\frac{dR_{\text{oxide}}}{dt} = \frac{1}{bX_{\text{oxide}} - X_E} D \left(\frac{\partial X}{\partial r}\right)\bigg|_{\text{interface}} \quad [10]$$

with all atomic percents referring to titanium in this paper.

To obtain the concentration gradient at the oxide/alloy interface, one must first solve the diffusion equation within the alloy subject to the relevant boundary conditions. The exact profile for an infinitely thick alloy film with one component forming an external oxide has been shown by Wagner[40] to be of the form $[X(r, t) - X_E]/[X_o - X_E] \sim \text{erf}\,[r/2(Dt)^{1/2}]$. This profile is shown schematically in Fig. 19a. To simply estimate the diffusion coefficient, we can approximate the profile as varying linearly from $X_E$ at the alloy/oxide interface to some distance $\Delta R$ within the alloy, at which point $X = X_o$, the initial composition of the alloy. This simplification of the profile is shown in Fig. 19b ($h \equiv$ film thickness). This linear approximation enables us to replace $(\partial X/\partial r)$ in Eq. 8 with $\Delta X_o/\Delta R$, defining $\Delta X_o \equiv X_o - X_E$, whereupon Eq. 8 becomes

$$\frac{dR_{\text{oxide}}}{dt} \approx \frac{D\Delta X_o}{(bX_{\text{oxide}} - X_E)\Delta R} \quad [11]$$

The parameter $\Delta R$ is the width of the depleted Ti zone in the alloy. $\Delta R$ can be calculated using mass conservation arguments simply by equating the amount of Ti depleted from the alloy to the amount required to create an oxide of width $R_{\text{oxide}}$

$$R_{\text{oxide}}(bX_{\text{oxide}} - X_o) = \frac{1}{2}\Delta R \Delta X_o \quad [12]$$

Substituting Eq. 9 into Eq. 10 and integrating yields a parabolic oxide growth rate

$$R^2_{\text{oxide}} = \frac{(\Delta X_o)^2}{(bX_{\text{oxide}} - X_E)(bX_{\text{oxide}} - X_o)} Dt \quad [13]$$

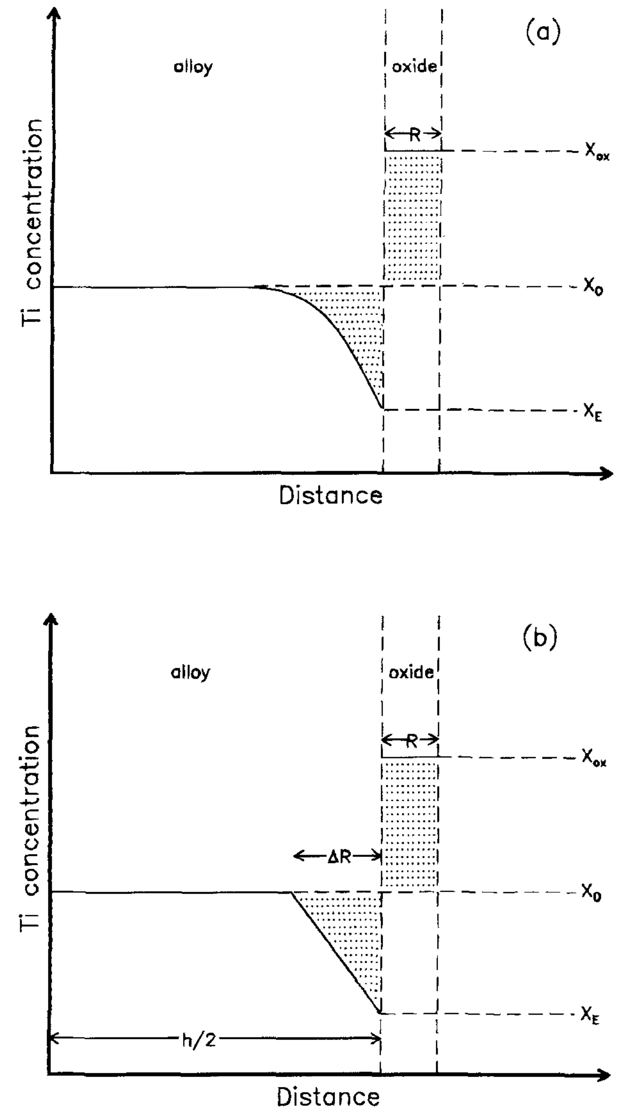


**Fig. 19. Concentration profile in an alloy below a growing oxide of one component only, (a) according to Wagner,[40] and (b) according to the linear approximation used in our model. Shaded areas are equal by mass conservation.**

which is of the form $R^2_{\text{oxide}} = k_R t$. Comparing Eq. 11 with Eq. 7, we can derive an expression for the variation of $k_x$ with the initial a/o Ti, $X_o$, in the alloy

$$k_x = \frac{4D(bX_{\text{oxide}} - X_o)(\Delta X_o)^2}{h^2(bX_{\text{oxide}} - X_E)} \quad [14]$$

In other words, $k_x$ can be fitted with a cubic equation, as was done in Fig. 18. Rather than do this, however, we manipulate Eq. 12 to a form which can be analyzed in a linear fashion

$$\left(\frac{k_x h^2}{bX_{\text{oxide}} - X_o}\right)^{1/2} = \left(\frac{4D}{bX_{\text{oxide}} - X_E}\right)^{1/2} \Delta X_o \quad [15]$$

If we plot $[k_x h^2/(bX_{\text{oxide}} - X_o)]^{1/2}$ *vs.* $X_o$, as in Fig. 20 for the four samples discussed (4, 5, 7.5, and 10 a/o Ti at 490°C), we can estimate the diffusion coefficient $D$ and $X_E$. Linear interpolation yields a slope of $\sim 1.2 \times 10^{-13}$ cm/s$^{1/2}$ and an $x$-intercept of $\sim 1.4$ a/o. The $x$-intercept from this linear fit corresponds to $X_E$ in Eq. 9, which is the concentration of Ti that remains in the alloy after oxidation. From Auger depth profiling, we measured this as $\sim 0.8$ a/o at 525°C (Fig. 7).

The slope of the linear fit is given by $[4D/(bX_{\text{oxide}} - X_E)]^{1/2}$, from which we can estimate the diffusion coefficient of Ti in Cu as $\sim 2.0 \times 10^{-13}$ cm$^2$/s at this temperature. Iljima *et al.* used a Matano-Boltzmann experiment to determine the diffusion coefficient of Ti in Cu as a function of composi-

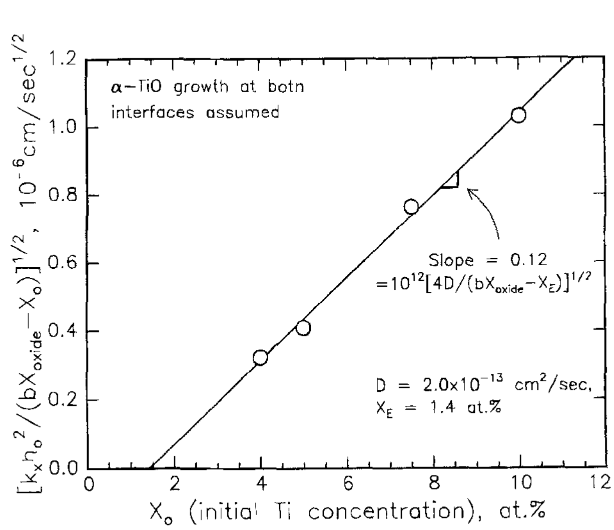


**Fig. 20. Concentration dependence of the reaction rate $k_x$ with initial Ti concentration according to Eq. 15 at 490°C. The slope is proportional to the diffusion coefficient of Ti in these alloys; the intercept to the Ti concentration remaining in the alloy.**

tion and temperature for highly dilute alloys.[41] Extrapolating from this work, we predict a value for the bulk diffusion coefficient of Ti in Cu of $\sim 4.0 \times 10^{-14}$ cm$^2$/s at 490°C, using the value for an infinitely dilute alloy. If we assume that $X_E$ is temperature independent, we can estimate $D$ as a function of temperature (Fig. 21) and compare the value so obtained to Iljima's data, also plotted in Fig. 21. The predicted values of $D$ are five to ten times greater than what is predicted by Iljima in this temperature range, which is reasonable given the approximations used to arrive at a diffusion coefficient for Ti in these alloy films.

## Conclusion

The reaction of $Cu_{1-x}Ti_x$ alloy films on $SiO_2$ for compositions of 4-10 a/o Ti is dominated by the dealloying of Ti to form oxides at both the free surface and at the $SiO_2$ interface. Segregation to each interface was apparent from both RBS and Auger depth profiling. The chemical state of the Ti varied at the free surface from $Ti_2O_3$ to TiO with increasing depth from the surface and consisted of TiO at the $SiO_2$ interface. Kinetics of dealloying are diffusion limited, with $X^2_{\text{Ti,reacted}} = k_x t$, as determined by *in situ* x-ray diffraction monitoring the Cu (111) peak and thereby the Cu lattice parameter. An activation energy of 1.6 ± 0.1 eV for this process was found for $Cu_{90}Ti_{10}$. By making certain simplify-

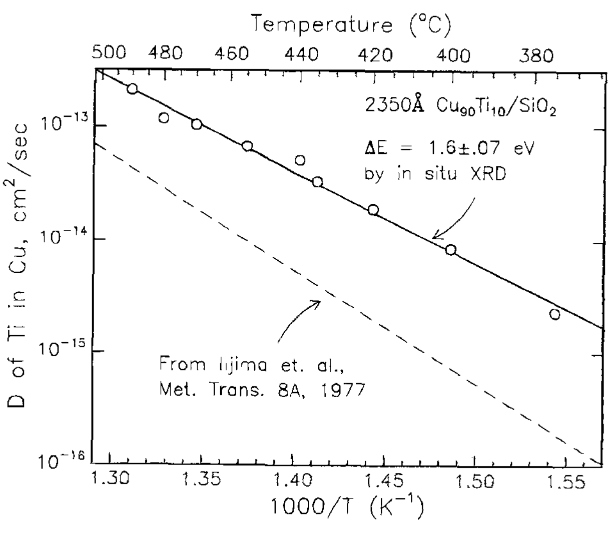


**Fig. 21. Arrhenius plot of our estimate of the diffusion coefficient of Ti in $Cu_{1-x}Ti_x$ alloy films. Dashed line is an extrapolation of data from Iljima *et al.*,[41] shown for comparison.**

ing assumptions, such as a linear gradient of Ti within the alloy, we establish that Ti diffusion out of the alloy rather than across the oxides is rate limiting and estimate the diffusion coefficient of Ti in these alloy films as $2 \times 10^{-13}$ $cm^2/s$ at 490°C.

## Acknowledgments

We would like to acknowledge partial support of this research by the Semiconductor Research Corporation. This work was also funded in part by the National Science Foundation (L. Hess, DMR-9307662 and L. Salmon, ECS-9410399). One of the authors (S. W. R.) would like to express his gratitude to the AT&T Corporation for a Ph.D. Scholarship during his graduate studies at Cornell. We gratefully appreciate the assistance and advice of Phil Chapman of the National Nanofabrication Facility at Cornell with Auger measurements and of Dr. Maura Weathers of the Materials Science Center X-Ray Facility at Cornell with XRD measurements.

Manuscript submitted July 29, 1994; revised manuscript received Nov. 29, 1994.

*Arizona State University assisted in meeting the publication costs of this article.*

REFERENCES

1. J. Li, Ph.D. Thesis, Cornell University, Ithaca, NY (1992).
2. J. Li, J. W. Mayer, and Y. Shacham-Diamand, *Mater. Sci. Rep.*, 9 (1992).
3. S. W. Russell, J. W. Strane, J. W. Mayer, and S. Q. Wang, *J. Appl. Phys.*, **76,** 257 (1994).
4. L. J. Brillson, M. L. Slade, H. W. Richter, H. VanderPlas, and R. T. Fulks, *J. Vac. Sci. Technol.*, **A4,** 993 (1986).
5. W. R. LaFontaine and C.-Y. Li, *Mater. Res. Soc. Symp. Proc.*, **203,** 163 (1991).
6. S. A. Rafalski, R. L. Spreitzer, S. W. Russell, T. L. Alford, J. Li, M. Moinpour, F. Moghadam, and J. W. Mayer, *ibid.*, **337,** 613 (1994).
7. R. L. Spreitzer, S. A. Rafalski, D. Adams, S. W. Russell, Z. Atzmon, J. Li, T. L. Alford, and J. W. Mayer, *ibid.*, **337,** 631 (1994).
8. Y. Shacham-Diamond, A. Dedhia, D. Hoffstetter, and W. G. Oldham, in *Proceedings of 8th International IEEE VLSI Multilevel Interconnection Conference,* p. 109, IEEE (1991).
9. Y. Shacham-Diamand, A. Dedhia, D. Hoffstetter, and W. G. Oldham, *This Journal,* **140,** 2427 (1993).
10. K. Hoshino, H. Yagi, and H. Tsuchikawa, *IEEE VMIC Conf. Proc.*, 226 (1989).
11. J. Li, J. W. Mayer, Y. Shacham-Diamond, and E. G. Colgan, *Appl. Phys. Lett.*, **24,** 2983 (1992).
12. J. Li, J. W. Mayer, and E. G. Colgan, *J. Appl. Phys.*, **70,** 2820 (1991).
13. D. Adams, R. L. Spreitzer, S. W. Russell, N. D. Theodore, T. L. Alford, and J. W. Mayer, *Mater. Res. Soc. Symp. Proc.*, **337,** 231 (1994).
14. J. L. Murray, in *Binary Alloy Phase Diagrams,* T. Massalski, Editor, pp. 970-972, American Society for Metals, Metals Park, OH (1986).
15. J. L. Liotard, D. Gupta, P. A. Psaras, and P. S. Ho, *J. Appl. Phys.*, **6,** 1895 (1985).
16. K. Hoshino, H. Yagi, and H. Tsuchikawa, in *Proceedings of 7th Intl. IEEE VLSI Multilevel Interconnection Conference,* p. 357, IEEE (1991).
17. R. E. Hummel, *Electronic Properties of Materials,* p. 78, Springer-Verlag, Berlin (1985).
18. S. W. Russell, J. Li, J. W. Strane, and J. W. Mayer, *Mater. Res. Soc. Symp. Proc.*, **260,** 763 (1992).
19. C. Kittel, *Introduction to Solid State Physics,* p. 144, John Wiley & Sons, Inc., New York (1986).
20. C. Cabral, Jr., J. M. E. Harper, K. Holloway, D. A. Smith, and R. G. Schad, *J. Vac. Sci. Technol.*, **A10,** 1706 (1992).
21. C.-J. Chen, C.-A. Chang, C. E. Farrell, and A. G. Schrott, *Appl. Phys. Lett.*, **62,** 654 (1993).
22. P. J. Ding, W. A. Lanford, S. Hymes, and S. P. Murarka, *J. Appl. Phys.*, **75,** 3627 (1994).
23. P. J. Ding, W. A. Lanford, S. Hymes, and S. P. Murarka, *Appl. Phys. Lett.*, **64,** 2897 (1994).
24. E. D. Zanotto and P. F. James, *J. Non-Cryst. Solids,* **104,** 70 (1988).
25. D. C. Rubie, Y. Tsuchida, T. Yagi, W. Utsumi, T. Kikegawa, O. Shimomura, and A. J. Brearley, *J. Geophys. Res.*, **95,** 15,829 (1990).
26. C. Marsh and H. Chen, *Acta Met.*, **38,** 2287 (1990).
27. R. A. Hamm and J. M. Vandenberg, *J. Appl. Phys.*, **56,** 293 (1984).
28. F. Sibieude and J. Rodriguez, *Thin Solid Films,* **204,** 217 (1991).
29. K. N. Tu, *J. Appl. Phys.*, **48,** 3400 (1977).
30. U. Köster, U. Schünemann, M. Blank-Bewersdorff, S. Brauer, M. Sutton, and G. B. Stephenson, *Mater. Sci. Eng.*, **A133,** 611 (1991).
31. W. Biegel, W. Schaper, H.-U. Krebs, J. Hoffmann, H. C. Freyhardt, R. Busch, and R. Bormann, *Colloque de Physique,* **C4,** 189 (1990).
32. J. S. Solomon and W. L. Baun, *Surf. Sci.*, **51,** 228 (1975).
33. C. Quenisset and R. Naslain, *Surf. Interface Anal.,* **13,** 130 (1988).
34. C. Apblett and P. J. Ficalora, *J. Appl. Phys.*, **69,** 4431 (1991).
35. D. R. Gaskell, *Introduction to Metallurgical Thermodynamics,* p. 287, Hemisphere Publishing Corporation, New York (1981).
36. G. E. Dieter, *Mechanical Metallurgy,* p. 50, McGraw-Hill, New York (1986).
37. *Journal of Physical and Chemical Reference Data,* M. W. Chase, Jr., C. A. Davies, J. R. Downey, Jr., D. J. Frurip, R. A. McDonald, and A. N. Syverud, Editors, **14,** p. 1658 for TiO, p. 1698 for $Ti_2O_3$, and p. 1721 for $Ti_3O_5$ (1985).
38. C. Y. Ting, M. Wittmer, S. S. Iyer, and S. B. Brodsky, *This Journal,* **131,** 2934 (1984).
39. S. W. Russell and S. Q. Wang, *J. Appl. Phys.,* **76,** 264 (1994).
40. C. Wagner, *This Journal,* **99,** 369 (1952).
41. Y. Iljima, K. Hoshino, and K.-I. Hirano, *Met. Trans. A,* **8A,** 997 (1977).